Contrib Mineral Petrol (2004) 146: 485–492
DOI 10.1007/s00410-003-0510-x

ORIGINAL PAPER

Aliouka Chabiron · Jacques Pironon
Dominique Massare

Characterization of water in synthetic rhyolitic glasses and natural melt inclusions by Raman spectroscopy

Received: 9 November 2002 / Accepted: 30 July 2003 / Published online: 24 October 2003

Abstract Raman spectroscopy was used to analyze quantitatively water in silicate glasses and melt inclusions and to monitor H_2O–OH speciation. Calibration is based on synthetic glasses with various water contents (0.02–7.67% H_2O); water determination and OH–H_2O differentiation on the area of the Si–O broad band at 468 cm^{-1} and the asymmetric O–H band at 3,550 cm^{-1}. Each Raman spectrum has been decomposed into four Gaussian + Lorentzian components centered at 3,330, 3,458, 3,560, and 3,626 cm^{-1} using the Levenberg–Marquardt algorithm. These components are interpreted to be two different types of H_2O molecule sites. The influence of the temperature on the loss of water is more important for molecular water than for the hydroxyl groups. The H_2O–OH partition confirms the typical evolution of water speciation in rhyolitic glasses as a function of the bulk water content. Method limitations have been studied for the application to natural melt inclusions.

Introduction

The quantity of dissolved volatiles (water, carbon dioxide ...) in magmas represents a key parameter for the understanding of igneous processes. The presence of water is known to drastically affect the chemical properties of magmas. The determination of the water content allows quantification of reaction rates, and a better understanding of crystal growth and mineral paragenesis. Addition of water to silicate melts leads to changes in their physical properties (Stolen and Walrafen 1976; Mysen et al. 1980; Stolper 1982a, 1982b), for example, a decrease in viscosity as a result of breaking oxygen bridges by insertion of OH groups, breakdown of Si–O lattices, and depolymerization. The determination of water content in natural silicate melts, therefore, is important to explain the P–T conditions of the genesis, ascent of magmas, and to characterize the type of the eruption. An estimation of the volatile and water contents in magmas are obtained through their determination in melt inclusions. These inclusions correspond to quantities of silicate melt that are trapped as defects into the lattice of a host mineral during the crystallization of the magma. Water content is conventionally determined in glasses by Karl–Fisher titration and manometry for bulk water content. Total H_2O content can be differentiated by thermo-gravimetric methods. However, the size of melt inclusions limits the application of such an analytical approach. Ion microprobe (Delaney and Karsten 1981; Deloule et al. 1995) and electron microprobe analyses (Devine et al. 1995; Morgan and London 1996) allow the determination of the total water content whereas infrared microspectroscopy permits quantification of molecular water and hydroxyl groups or silanols (Stolper 1982a, 1982b; Newman et al. 1986; Silver et al. 1990; Behrens et al. 1996; Salova et al. 1996). However, these techniques have some limitations: ion microprobe is destructive and not a routine technique, electron microprobe gives an indirect water concentration estimate by subtracting the sum of the analyzed elements from 100%, and infrared spectroscopy requires a 20-μm diameter area and an adequate sample preparation (glass inclusion must be exposed on both surfaces of a doubly polished wafer thin section and inclusion thickness must be known) (Stolper 1982a; Newman et al. 1986; Ihinger et al. 1994; Zhang et al. 1997). Raman microspectroscopy has been recently used to characterize melt inclusions. Although used for the understanding of the structures of glass and melt (Brawer and White 1975; Matson et al. 1983; McMillan 1984; Galeener

Editorial responsibility: T.L Grove

A. Chabiron · J. Pironon (✉)
CREGU-UMR G2R 7566, BP 239,
54506 Vandoeuvre-lès-Nancy, France
E-mail: Jacques.Pironon@g2r.uhp-nancy.fr
Tel.: +3-83-684732
Fax: +3-83-684701

D. Massare
Laboratoire Pierre Süe, CEN/Saclay,
91191 Gif sur Yvette cedex, France

1985), Raman spectroscopy was rarely used for quantitative analysis of water in melt inclusions. Chabiron et al. (1999) developed a quantitative application of the Raman spectrometry to determine the water concentrations of melt inclusions. Thomas (2000) determined water content in granitic melt inclusions by confocal laser Raman spectroscopy. This technique has great potential: (1) it is non-destructive, (2) it does not require complex sample preparation, and (3) it has a high spatial resolution (the diameter of the laser spot is near one micrometer). Fluorescence of the sample is sometimes a limitation, masking the Raman scattering of glasses. The objectives of this work are first to determine an adequate analytical procedure for melt inclusions and second to delineate H_2O–OH speciation in glasses. Raman spectroscopy has been calibrated using synthetic glasses with well-known water contents.

Samples

Nine synthetic rhyolitic glasses (six produced at CREGU and Clermont-Ferrand laboratories and three provided by Withers and Behrens 1999) and two synthetic SiO_2 glasses (Heraeus, France) were used as standards for the calibration of the Raman spectroscopy.

Samples with low water-contents were two thin slides of Suprasil I and Herasil I (Heraeus, France) containing less than 1,000 and 150 ppm of water, respectively.

Synthetic glasses AC1, AC2, AC3, AC4, AC5, and AC6 were synthesized from high purity SiO_2, Na_2CO_3, K_2CO_3, and Al_2O_3 reagents. Na_2CO_3 and K_2CO_3 were heated to 1,000 °C to drive off CO_2 and H_2O. Oxide powders were mixed in desired proportions to produce a rhyolitic composition. Weighed powders were loaded into gold capsules with one end welded shut along with a pre-weighed amount of distilled water then welded shut. Capsules were loaded into an internally heated pressure vessel and run at 950 °C and 4,000 bar for 48 h. Samples were quenched by drop of temperature. Homogeneity of the glasses was examined by microscopy and confirmed by Raman microspectroscopy. Water content of the reference glasses was analyzed by Karl Fisher titration with analytical error below 2% (CRPG, Nancy, France).

Three volcanic glasses trapped in quartz crystals of pumice falls were selected according to their composition (Table 1) and their geological context. We have chosen quenched material such as pumice falls to avoid post-entrapment crystallization on the walls of the cavity, which occurs during slow cooling of lava flows. All inclusions are completely glassy at room temperature without any shrinkage bubble. San Pietro (Sardinia, Italy, 14 million years) has a peralkaline comenditic composition with moderate iron and alkali contents ($\sum Na_2O + K_2O > 8$ wt%) (Larhidi 1981). Melt inclusions in quartz from Guadeloupe (Lesser Antilles, 250,000 years) come from a calc-alkaline subduction-related suite and are metaluminous rhyolitic in composition (Clocchiatti 1975). Melt inclusions in quartz from the Mont Dore (La Bourboule, French Massif Central, 3 million years old) come from an alkaline continental series.

Analytical techniques

Fourier transform infrared spectroscopy

Water content in melt inclusions were analyzed by Fourier transform infrared spectroscopy (FTIR). The FTIR measurements were performed using a Nicolet Magna IR550 spectrometer equipped with a global source, a MCT/A detector cooled with liquid N_2, a KBrXT beam splitter, coupled with a Spectra Tech microscope. Considering the high water content of the melt inclusions, combination bands at 5,230 (H_2O) and at 4,500 cm^{-1} (OH) were used for the quantification of water in glass. The chosen extinction coefficients for the

Table 1 Average compositions and standard deviations of silicate glasses (AC1, AC2, AC3, AC4, AC5, AC6) and melt inclusions from Mont Dore, Guadeloupe, and San Pietro. – Not analyzed. *M. Dore* Mont Dore; *Guadel.* Guadeloupe; *S. Pietro* San Pietro

Compositions of silicate glasses and melt inclusions																		
Location	M. Dore		Guadel.		S. Pietro		AC1		AC2		AC3		AC4		AC5		AC6	
Element	(wt%)	σ	(wt%)	σ	(wt%)	σ	(wt%)	σ	(wt%)	σ	(wt%)	σ	(wt%)	σ	(wt%)	σ	(wt%)	σ
SiO_2	71.78	0.04	71.73	1.09	70.65	1.36	68.74	0.67	69.04	1.15	69.74	0.61	69.47	1.23	67.70	1.06	67.65	0.61
TiO_2	0.11	0.02	0.25	0.10	0.12	0.10	-	-	-	-	-	-	-	-	-	-	-	-
Al_2O_3	11.55	0.12	11.56	0.14	10.02	0.27	13.02	0.10	13.41	0.08	14.65	0.08	14.13	0.22	13.18	0.14	12.31	0.17
FeO	0.72	0.05	1.07	0.19	2.78	0.32	-	-	-	-	-	-	-	-	-	-	-	-
MnO	0.04	0.02	0.10	0.20	0.10	0.10	-	-	-	-	-	-	-	-	-	-	-	-
MgO	0.04	0.01	0.09	0.10	0.06	0.02	-	-	-	-	-	-	-	-	-	-	-	-
CaO	0.27	0.00	0.79	0.13	0.08	0.05	-	-	-	-	-	-	-	-	-	-	-	-
Na_2O	3.87	0.17	3.14	0.17	4.66	0.22	6.05	0.12	5.51	0.12	4.94	0.21	4.74	0.24	5.43	0.18	5.49	0.59
K_2O	4.39	0.35	3.18	0.20	4.17	0.20	6.52	0.19	5.93	0.17	5.11	0.11	5.10	0.29	5.77	0.22	5.99	0.29
Cl	0.30	0.01	0.25	0.06	0.45	0.03	-	-	-	-	-	-	-	-	-	-	-	-
Total	93.05	0.49	92.16	2.38	93.09	2.67	94.33	0.77	93.89	1.30	94.44	0.56	93.44	1.47	92.08	0.97	91.44	0.93
H_2O[a]	-	-	-	-	-	-	3.19	< 0.06	3.70	< 0.07	3.73	< 0.07	4.61	< 0.09	5.97	< 0.12	7.67	< 0.15

[a]Water concentration by Karl Fisher analysis (error < 2%)

calculation were 1.86 and 1.50 l mol^{-1} cm^{-1}, respectively (Ihinger et al. 1994). The thickness of the sample was measured and for the biggest samples (≥0.5 mm^3) the density was determined by flotation. The sample was placed in a sodium metatungstate solution with a density of 3 g ml^{-1}. Pure water was added until the sample remained in equilibrium with the solution and decreased in density. The sample density, therefore, was considered to be equal to the density of the solution. An average density of 2.34 g cm^{-3} was used for the calculation.

Raman spectroscopy

The water analysis in glasses and melt inclusions was obtained using a Labram Dilor microspectrometer at CREGU laboratory, Nancy, France. A grating of 600 was used and allowed us to record spectra between 100 and 4,000 cm^{-1}, covering, in one experiment, the area of the silicate framework at low wave numbers and the area of the water-stretching bands at high wave numbers. An Olympus optical microscope with a long distance 80x objective was used. A CCD detector collected glass spectra with sample excitation produced by an argon laser beam (514.5 nm) at a power of 300 mW and an acquisition time of 1 min. The Raman analysis does not require abnormal preparation of the sample. The Raman spectrometer is equipped with a Linkam microthermometric stage. Spectra have been recorded up to 400 °C. At higher temperatures, the intensity of the Raman signal decreases and does not allow accurate measurement.

Raman spectra of hydrous rhyolitic glasses

Band assignments

Si–O vibration modes correspond to a broad band at 468 cm^{-1} (bending) and to a weak contribution near 1,100 cm^{-1} (stretching, see Fig. 1). The band at 776 cm^{-1} is assigned to Si–O–Si bending vibrations. Hydroxyl group [Si(Al)–OH] are located between 900–1,000 cm^{-1} for the bending mode and at ~3,500 cm^{-1} for the stretching mode. Molecular water contribution is detected at 1,620 cm^{-1} (bending) and between 3,200 and 3,450 cm^{-1} (stretching; Brawer and White 1975; Mysen et al. 1982; Matson et al. 1983; McMillan 1984). The Raman spectrum varies with water content. The Raman spectrum of Suprasil 1 with 1,000 ppm of OH shows a weak asymmetric band near 3,500 cm^{-1} due to the O–H stretching vibration of hydroxyl groups. The only or dominant hydrous species present in low-water content silicate glasses are hydroxyls (Stolen and Walrafen 1976; Stolper 1982b; McMillan and Remmele 1986). In the water-rich glasses, the O–H stretching zone is broader than in low-water content glasses and extends from 3,000 to 3,800 cm^{-1}. This is due to the presence of molecular H_2O.

Spectral treatment

Acquired spectra require a baseline correction in most cases because of luminescence and/or fluorescence of glass under laser radiation. The method for water determination and OH and H_2O differentiation in glasses is based on the area calculation of the asymmetric OH stretching band between 3,000 and 3,788 cm^{-1} and on the asymmetric Si–O broad band between 228 and 554 cm^{-1}. A test of repeatability has been made on one natural melt inclusion from the Mont-Dore rhyolite (Table 2). The error (1σ) on water determination is 1.1% and combines acquisition and treatment errors.

For our reference glasses, the second derivative of the spectra produces four main band contributions. By consequence, each spectrum has been decomposed into four Gaussian + Lorentzian components centered at 3,330, 3,458, 3,560, and 3,626 cm^{-1} using the

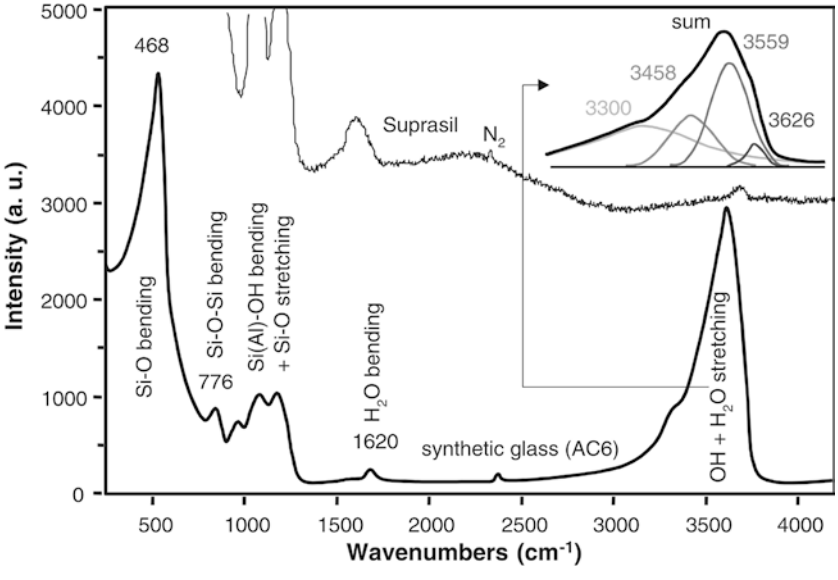

Fig. 1 Raman spectrum of synthetic glass (AC6) containing 7.67 wt% H_2O with the location of the different typical bands of water (1,620 and 3,560 cm^{-1}), Si–O, Si–O–Si, and Si(Al)–OH. The Raman spectrum of Suprasil 1 glass with less than 1,000 ppm H_2O is shown for comparison

Table 2 Raman spectroscopy data (Si–O, OH + H_2O band areas, (OH + H_2O)/Si–O band area ratio and % H_2O (calculated from calibration equation) from 11 analyses on the same location of one melt inclusion from Mont Dore showing the good repeatability of the Raman analysis

Repeatability of the Raman analysis				
Raman spectrum	SiO (10^6)	OH + H_2O (10^6)	OH + H_2O/SiO	wt% H_2O R[a]
1	3.63482	2.89077	0.79530	5.01
2	3.59632	2.86990	0.79801	5.03
3	3.63975	2.82860	0.77714	4.90
4	3.59831	2.83540	0.78798	4.96
5	3.62143	2.89965	0.80069	5.04
6	3.62999	2.87109	0.79094	4.98
7	3.61217	2.87051	0.79468	5.01
8	3.60981	2.81236	0.77909	4.91
9	3.61261	2.79540	0.77379	4.87
10	3.59963	2.82942	0.78603	4.95
11	3.61486	2.84376	0.78669	4.96
Average	3.61543	2.84971	0.78821	4.97
σ	0.01474	0.03304	0.00879	0.06
% error	0.40781	1.15957	1.11483	1.11

[a]Water concentration obtained by Raman spectroscopy

Levenberg–Marquardt algorithm (Fig. 1). We interpret these four components as due to two different types of OH oscillators with different vibration modes. This decomposition is in agreement with that of Mysen et al. (1997), who showed that the band at 3,550 cm^{-1} may be the result of three main bands at 3,350, 3,500, and 3,575 cm^{-1} and an additional weak band around 3,640 cm^{-1}. Spectral treatments have been done with OPUS software (Bruker).

Results and discussion

Calibration of the Raman technique

The calibration of the Raman technique was made using synthetic glasses with different, known water contents. It was based on the correlation between the known water content determined by the Karl Fisher titration and the ratio of the areas of the H_2O + OH stretching band and the Si–O bending band (Table 3). Each point corresponded to the mean of three determinations ($\pm 1\sigma$ standard deviation). A linear relationship was obtained (Fig. 2). This regression allows determination of dissolved water contents in glasses from the H_2O + OH stretching band to Si–O bending band ratio:

$$\text{Water content } (\%) = [H_2O + OH]^{Area}/[Si - O]^{Area} \times 6.3$$
$$\text{with } r^2 = 0.96,\ n = 11$$

Differences between the two methods could be possible because Karl Fisher is a bulk technique whereas Raman is a micro-technique. These results demonstrate that Raman spectroscopy can be easily used to determine the dissolved water content in glasses.

Comparison with infrared water data

Measurements of dissolved H_2O by Raman spectrometry were applied to natural melt inclusions from Mont Dore, Guadeloupe, and San Pietro and compared with determinations by infrared micro-spectrometry. Infrared data and Raman results are given in Table 4. For melt inclusions with the highest water contents, Raman water contents are similar to those obtained by infrared spectroscopy with differences less than 10% for MD 25 and G51-9A, and about 10% for SP 1 and G51-1. For the other melt inclusions, differences between water content analyzed by Raman spectroscopy and water content, when analyzed by infrared spectroscopy, may be up to 27%. Raman results show a good homogeneity for each location whereas dispersion of infrared data is ~10%. Different error types can affect water determination by Raman and infrared micro-spectrometry. Infrared data are mainly affected by the thickness, the signal/background ratio, and by baseline correction. FTIR allows several water determinations: total H_2O from measurements at 7,100 and 3,570 cm^{-1} (an interesting method for low-water concentration glasses), molecular water from measurement at 1,630 cm^{-1}, and the water speciation by the measurement of the absorption bands at

Table 3 Raman spectroscopy data obtained on synthetic glasses used for calibration of water determination: Si–O, OH + H_2O average band areas and (OH + H_2O)/Si–O band area ratio and its standard deviation are noted. For each sample, the laser beam has been focused on three different locations. Weight % H_2O corresponds to concentrations determined by Karl Fisher analysis

Raman spectroscopy data for calibration of water determination					
Sample	Karl Fisher	Raman micro-spectrometry			σ
	% H_2O	SiO (10^6)	OH + H_2O (10^6)	OH + H_2O/SiO	
AC6	7.67	3.78750	5.08375	1.348	0.018
AC5	5.97	8.33000	6.97667	0.838	0.037
KS52	5.20	10.86667	9.35333	0.861	0.027
AC4	4.61	7.60667	5.54667	0.729	0.162
AC3	3.73	9.43000	5.49000	0.582	0.061
AC2	3.70	8.67667	4.62000	0.532	0.048
KS32	3.20	8.45000	4.74000	0.561	0.061
AC1	3.19	9.74667	3.63667	0.373	0.032
KS12	1.20	8.02000	2.02327	0.252	0.016
S1	0.10	12.13333	0.01671	0.001	0.000
H1	0.02	11.96667	0.01565	0.001	0.000

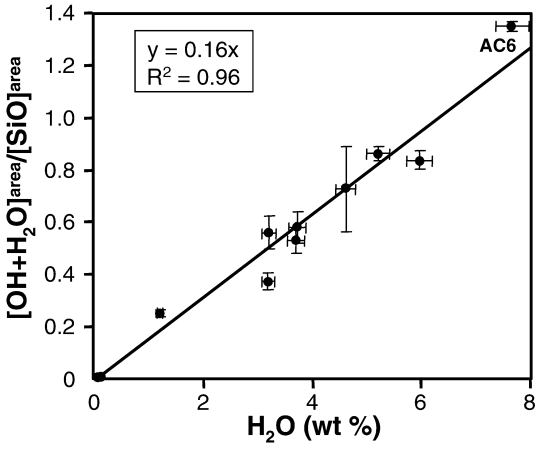

Fig. 2 Calibration curve for the determination of water content in glasses: referenced water content vs. (OH + H_2O)/Si–O band area ratio. These values correspond to those noted in Table 1. A linear relationship is obtained, allowing for the determination of the dissolved water content in glasses from the H_2O + OH stretching band/Si–O bending band ratio: water content (%) = $[H_2O+OH]^{Area}/[Si-O]^{Area} \times 6.3$ with $r^2 = 0.96$, n = 11

4,500 cm^{-1} for OH and 5,230 cm^{-1} for H_2O, whereas Raman routine water estimation does not split OH and H_2O contributions. Raman data are sensitive to luminescence, depth of inclusion, and quartz spectrum subtraction. However, an attempt at Raman spectrum decomposition has been made to monitor OH/H_2O speciation with temperature.

Limitations

Luminescence

Luminescence of a melt inclusion under visible laser excitation is induced by the presence of trace elements in natural glasses or by defects in the silicate lattice. Tests of repeatability indicate an error on the area calculation of the OH + H_2O stretching band that is three times higher than on the area calculation of the Si–O bending band (Table 1). This difference can be explained by a baseline treatment that is generally more important for OH– than for the Si–O band. The luminescence of the melt inclusion implies a differential baseline treatment with wave numbers. The area calculation will be more affected in the high wave-number region because luminescence intensity of an argon laser increases with the wave numbers in the considered spectral range. This luminescence can be lowered by recording spectra at a temperature of ~60 °C. Such a temperature is considered to have no effect on water content.

Effect of quartz: spectra treatment

Water can be determined by Raman spectroscopy in melt inclusions located at the surface or at different depths of the quartz-hosted phenocrysts. Even if confocal Raman equipment is used, the melt inclusion analysis needs a specific treatment to delete the effect of the quartz matrix. The quartz host is also analyzed by Raman spectroscopy in the neighborhood of the inclusion and its spectrum must be subtracted from the Raman spectrum of the melt inclusion. The bending vibrations from quartz are superimposed on bending Si–O vibrations from glass. The residual Raman spectrum corresponds to the melt inclusion spectrum without the host mineral contribution. This subtraction, executed using the Opus software, can contribute to the error of water concentration calculation.

Effect of depth of melt inclusion in the quartz host

We analyzed different melt inclusions with homogeneous water contents hosted by quartz located at different depths between the surface and a depth of 136 μm. Figure 3 shows that the ratio of the H_2O + OH stretching band area and the Si–O bending band area decreases with increasing depth to the melt inclusion. It appears that, down to 119 μm depth, the water content

Table 4 Raman and FT-IR spectroscopy data obtained on natural melt inclusions from Mont Dore (MD), San Pietro (SP), and Guadeloupe (G): SiO, OH + H_2O band areas and (OH + H_2O)/Si–O band area ratio, %Water (R) corresponds to calculated bulk water content from Raman calibration equation [Water content (wt%) = $[H_2O + OH]^{Area}/[Si–O]^{Area}$x6.3], Abs. 5230 and Abs. 4,500 correspond to the measured infrared absorbances of the H_2O and OH functional groups, respectively, thickness of each inclusion has been measured; %water (ir) corresponds to calculated bulk water content from the Beer–Lambert's law

Comparison between water concentrations obtained by Raman spectroscopy and FTIR

Sample	Location	SiO (10^6)	OH + H_2O (10^6)	OH + H_2O/SiO	%Water (R)[a]	Abs. 5,230 cm^{-1}	Abs. 4,500 cm^{-1}	Thickness (μm)	%Water[b] (ir)
MD 25	Mont Dore	3.63482	2.89077	0.795	5.01	0.111	0.0236	115	5.00
SP 1	San Pietro	6.10966	2.90692	0.476	3.00	0.0444	0.0096	70	3.31
SP 2	San Pietro	7.37822	3.55020	0.481	3.03	0.092	0.0214	131	3.71
SP 3	San Pietro	7.05822	3.30700	0.469	2.95	0.111	0.0247	154	3.76
G51-9A	Guadeloupe	7.72676	5.91363	0.765	4.82	0.104	0.0306	124	4.69
G51-1	Guadeloupe	7.62970	5.83678	0.765	4.82	0.0524	0.0203	73	4.32

[a]Water concentration determined by Raman spectroscopy
[b]Water concentration determined by FTIR

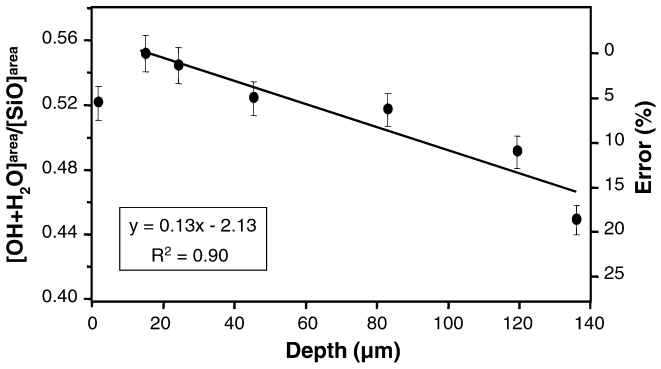

Fig. 3 Depth of melt inclusion (μm) vs. $[OH + H_2O]^{Area}/[Si–O]^{Area}$ diagram (between the surface and 136 μm depth), showing that the ratio of the H_2O + OH stretching band area and the Si–O bending band area decrease with increasing depth of the melt inclusion location. Up to 90 μm in depth, inclusions present correct water concentrations with lower than 10% error in comparison to the value obtained on an inclusion at low depth

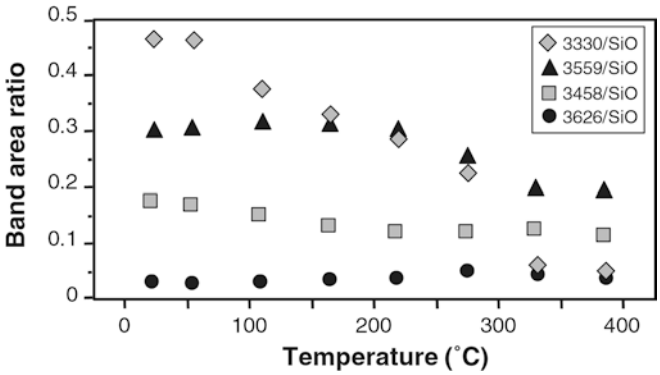

Fig. 4 Temperature vs. (decomposed H_2O band)/Si–O (3,330, 3,458 cm^{-1}) and temperature vs. (decomposed OH band)/Si–O (3,559, 3,626 cm^{-1}) diagrams. The influence of temperature on the loss of water from rhyolitic glass is more important for molecular water than for hydroxyl groups, and is more stable in the glass structure below 400 °C

decrease is lower than 10% compared with the value obtained in an inclusion at the surface. Nevertheless, inclusions at the surface result in a lower water content than inclusions at depth. However, the water content in inclusions at the surface does not represent the real water concentration of the natural glass because of possible dehydration. The reduction in the ratio of the H_2O + OH stretching band area and the Si–O bending band area is due to the slightly different behavior of the H_2O band and the Si–O band. The intensity of the H_2O band decreases more than the intensity of the Si–O band. This phenomenon can be explained by the variation in optical transmission as a function of the wavelength through the quartz crystal.

The concentration obtained for an inclusion at low depths of ~15 μm is more representative of the real water concentration. For depths less than 15 μm, the error increases. Down to 90-μm depth, inclusions yield correct water concentrations with less than 10% error compared with the value obtained for an inclusion at less depth.

Effect of quartz orientation

The band area ratio was measured on glass inclusions in quartz at 10 μm below the surface using a rotational stage and double polarization. Measurements were made at each 15° without polarizors. Angles of 0 and 90° correspond to quartz pseudo-extinction. Slight variations in the band area ratio were observed, which do not exceed 10%. The ratio was weaker at 45° to the extinction angle.

Temperature effect on the water content of glasses

Figure 4 illustrates the temperature dependence of the ratio of each decomposed band area from the H_2O + OH stretching band and the Si–O bending band area. The ratio of the decomposed band at 3,330 cm^{-1} and the Si–O band is constant up to 60 °C. From 110 to 275 °C, (heating rate 5 °C min^{-1}), this ratio significantly and regularly decreases. After 300 °C, it strongly decreases. At 385 °C, the 3,330 band looses about 89% of its integrated intensity. The decrease in the ratio of the decomposed band area centered at 3,458 cm^{-1} to the Si–O band area decreases from 60 to 385 °C by approximately 34% relative to room temperature. The ratio of the decomposed band area at 3,559 cm^{-1} and the Si–O band is quite constant up to 220 °C and then decreases by about 36%. The ratio of the decomposed band area at 3,626 cm^{-1} and the Si–O band is constant with increasing temperature. The influence of temperature on the loss of water from rhyolitic glass is more important for molecular water than for hydroxyl groups, which are more stable in the glass structure below 400 °C. However, an attempt at Raman spectrum decomposition has been made to monitor OH/H_2O speciation with temperature.

OH/H_2O speciation

Samples AC5 and AC6 were analyzed by Raman spectroscopy at different temperatures from 20 to 385 °C. The results indicate a loss of bulk water content with increasing temperature. The ratio of the H_2O + OH stretching band area and the Si–O bending band area was used with the calibration curve to obtain the bulk water content of the glass at each temperature. Each spectrum was then decomposed as explained above. The sums of the area of the two decomposed bands corresponding to molecular water (3,330 and 3,458 cm^{-1}) and the sum of the area of the two decomposed bands corresponding to hydroxyl groups (3,559 and 3,626 cm^{-1}) were calculated. Figure 5 shows the area ratio of the molecular water and the Si–O band and the hydroxyl groups and the Si–O band as a function of bulk water

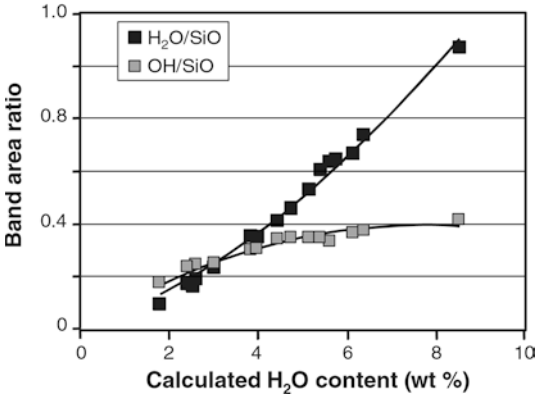

Fig. 5 Differentiation of molecular water and hydroxyl groups in calculated water vs. OH/Si–O or H_2O/Si–O area ratios diagram for the AC5 and AC6 glasses. The bulk water content is determined from the calibration curve shown in Fig. 2. At low bulk water, most of the water is dissolved as hydroxyl groups in glass. At bulk water of about 3 wt%, equal amounts of water are dissolved as molecular water and hydroxyl groups. For a bulk water content higher than ~3 wt%, most of the water is dissolved as molecular water

for the AC5 and AC6 glasses. The cross sections of hydroxyls and water are considered equivalent.

At low bulk water content, most of the water is dissolved as hydroxyl groups in glass. At a bulk water content of approximately 3 wt%, equal amounts of water are dissolved as molecular water and hydroxyl groups. For bulk water contents higher than ~3 wt%, most of the water is dissolved as molecular water. The hydroxyl group content becomes relatively constant or slightly increases, whereas the molecular water concentration rapidly increases.

These results show the typical evolution of water speciation in rhyolitic glasses as a function of bulk water content (Stolper 1982b; Newman et al. 1986; Silver et al. 1990; Schmidt et al. 2001). The inflection point of 3 wt% of bulk water content is in good agreement with the data of Silver et al. (1990) and Ihinger et al. (1999), obtained on rhyolitic glasses synthesized in rapid quench cold seal bombs by infrared spectroscopy, and with the data of Schmidt et al. (2001) on aluminosilicate glasses with NMR spectroscopy.

Conclusions

This study demonstrates the potential of Raman spectroscopy for quantitative analysis of dissolved water in silicate glasses and in rhyolitic melt inclusions over the H_2O concentration range 0.2–7.7 wt%. Raman spectroscopy allows for analyses of melt inclusions that are < 20 μm in diameter (up to 5–10 μm), which cannot be analyzed by transmission infrared spectroscopy due to their small size.

Raman spectroscopy has been calibrated using synthetic glasses with well-known water contents determined by the Karl Fisher method. The obtained calibration curve permits the determination of total dissolved water contents in glasses or natural melt inclusions and the monitoring of H_2O–OH speciation in glasses.

In addition, the study of the effects of luminescence, quartz matrix, depth of melt inclusion in quartz, and quartz orientation allowed us to determine an adequate analytical procedure for melt inclusions. First, subtraction of the quartz Raman spectrum from the melt inclusion Raman spectrum is required. Second, the choice of a melt inclusion at a depth of about 15 μm is recommended. Inclusions at the surface are water re-equilibrated with the atmosphere and are not totally representative of the initial water content of melt. For inclusions at greater depths, a correction should be applied for water estimation. Third, recording spectra at around 60 °C without effecting the dissolved water content can lower the luminescence. Finally, variations of the band area ratio due to the rotation angle of quartz did not exceed 10%. Thus, the adequate analytical procedure for melt inclusions does not require particularly complex sample preparation techniques. The standard deviation derived from the calibration curve is probably due to the difficulty in comparing results obtained from a micro-technique with standard reference materials that have been characterized by a bulk technique.

Furthermore, it is interesting to examine the water re-equilibration phenomenon between atmosphere and melt inclusion when the melt inclusion is at the surface of the host mineral. More systematical analyses of the same melt inclusions at different depths and at the surface in various atmosphere conditions (hydrous, dried) would help us to understand this phenomenon. It has serious implications for the preparation and storage of melt inclusions. In addition, this method allows for the analyses of small inclusions, in particular mantel inclusions smaller than 20 μm. Compared with Thomas (2000), this work determines the limits of Raman spectroscopy and describes the methodological cautions needed to determine bulk water content in natural melt inclusions. Further studies should focus on stretching the water band decomposition. It could become possible to quantify hydroxyl groups and molecular water using Raman micro-spectrometry.

Acknowledgements The authors wish to thank R. Clocchiatti (CEN/Saclay, France) for helpful discussions and for providing samples from Mont Dore, San Pietro, and Guadeloupe; C. Peiffert (CREGU, France) and F. Gibert (Université de Clermont-Ferrand, France), respectively, for the preparation and for heating the standard glasses.

References

Behrens H, Romano C, Nowak M, Holtz F, Dingwell DB (1996) Near-infrared spectroscopic determination of water species in glasses of the system MalSi3O8 (M = Li, Na, K): an interlaboratory study. Chem Geol 128:41–63

Brawer SA, White WB (1975) Raman spectroscopic investigation of silicate glasses. I. The binary alkali silicates. J Chem Phys 63:2421–2432

Chabiron A, Peiffert C, Pironon J, Cuney M (1999) Determination of water content in melt inclusions by Raman spectrometry. In: Ristedt H (ed) Lüders V, Thomas R, Schmidt-Mumm A (eds) ECROFI XV (European Current Research on Fluid Inclusions), Abstr Prog., Terra Nostra — Schr Alfred-Wegner-Stiftung 99/6, pp 68–69

Clocchiatti R (1975) Les inclusions vitreuses des cristaux de quartz. Etude optique, thermo-optique et chimique. Applications géologiques. Mem Soc Géol France

Delaney JR, Karsten JL (1981) Ion microprobe studies of water in silicate melts: concentration-dependent water diffusion in obsidian. Earth Planet Sci Lett 52:192–202

Deloule E, Paillat O, Pichavant M, Scaillet B (1995) Ion microprobe determination of water in silicate glasses: methods and applications. Chem Geol 125:19–28

Devine JD, Gardner JE, Brack HP, Layne GD, Rutherford M (1995) comparison of microanalytical methods for estimating H_2O contents of silicic volcanic glasses. Am Mineral 80:319–328

Galeener FL (1985) Raman and ESR studies of the thermal history of amorphous SiO_2. J Non-Cryst Solids 71:373–386

Ihinger PD, Hervig RL, McMillan PF (1994) Analytical methods for volatiles in glasses. In: Carroll MR, Holloway JR (eds) Volatiles in magmas. Rev Mineral 30:67–121

Ihinger PD, Zhang Y, Stolper EM (1999) The speciation of dissolved water in rhyolitic melt. Geochim Cosmochim Acta 63:3567–3578

Larhidi N (1981) Contribution à l'étude des laves hyperalcalines de l'île de S.Pietro (Sardaigne). Thèse 3ème cycle, Paris-Orsay

Matson DW, Sharma SK, Philpotts JA (1983) The structure of high-silica alkali-silicate glasses — a Raman spectroscopic investigation. J Non-Cryst Solids 58:323–352

McMillan P (1984) Structural studies of silicate glasses and melts — applications and limitations of Raman spectroscopy. Am Mineral 69:622–644

McMillan PF, Remmele RL (1986) Hydroxyl sites in SiO_2 glass: a note on infrared and Raman spectra. Am Mineral 71:772–778

Morgan GB VI, London D (1996) Optimizing the electron microprobe analysis of hydrous alkali aluminosilicate glasses. Am Mineral 81:1176–1185

Mysen BO, Virgo D, Scarfe CM (1980) Relations between the anionic structure and viscosity of silicate melts: a Raman spectroscopic study. Am Mineral 65:690–710

Mysen BO, Virgo D, Seifert FA (1982) The structure of silicate melts: implications for chemical and physical properties of natural magma. Rev Geophys Space Phys 20:353–383

Mysen BO, Holtz F, Pichavant M, Beny J-M, Montel J-M (1997) Solution mechanisms of phosphorous in quenched hydrous and anhydrous granitic glass as a function of peraluminosity. Geochim Cosmochim Acta 61:3913–3926

Newman S, Stolper EM, Epstein S (1986) Measurement of water in rhyolitic glasses: calibration of an infrared spectroscopic technique. Am Mineral 71:1527–1541

Salova TP, Epel'baum MB, Stolyarova TA, Zavel'sky VO (1996) Relationship between molecular water and hydroxyl groups in rhyolitic and quartz glasses. Chem Erde 56:383–386

Schmidt BC, Berhrens H, Riemer T, Kappes R, Dupree R (2001) Quantitative determination of water speciation in aluminosilicate glasses: a comparative NMR and IR spectroscopic study. Chem Geol 174:195–208

Silver LA, Ihinger PD, Stolper E (1990) The influence of bulk composition on the speciation of water in silicate glasses. Contrib Mineral Petrol 104:142–162

Stolen RH, Walrafen GE (1976) Water and its relation to broken bond defects in fused silica. J Chem Phys 64:2623–2631

Stolper E (1982a) Water in silicate glasses: an infrared spectroscopic study. Contrib Mineral Petrol 81:1–17

Stolper E (1982b) The speciation of water in silicate melts. Geochim Cosmochim Acta 46:2609–2620

Thomas R (2000) Determination of water contents of granite melt inclusions by confocal laser Raman microprobe spectroscopy. Am Mineral 85:868–872

Withers AC, Behrens H (1999) Temperature induced changes in the NIR spectra of hydrous albitic and rhyolitic glasses between 100 and 300 K. Phys Chem Mineral 27:119–132

Zhang Y, Belcher R, Ihinger PD, Wang L, Xu Z, Newmann S (1997) New calibration of infrared measurement of dissolved water in rhyolitic glasses. Geochim Cosmochim Acta 5:3089–3100